bioRxiv preprint doi: https://doi.org/10.1101/2020.03.29.013342; this version posted April 9, 2020. The copyright holder for this preprint (which was not certified by peer review) is the author/funder, who has granted bioRxiv a license to display the preprint in perpetuity. It is made available under aCC-BY-NC-ND 4.0 International license.

A one-enzyme RT-qPCR assay for SARS-CoV-2, and procedures for reagent production

Sanchita Bhadra, Andre C. Maranhao, and Andrew D. Ellington[1]

Center for Systems and Synthetic Biology
University of Texas at Austin
Austin, TX
78703

[1] Inquiries about manuscript to ellingtonlab@gmail.com
[2] Inquiries about vectors to a.maranhao@utexas.edu

ABSTRACT

Given the scale of the ongoing COVID-19 pandemic, the need for reliable, scalable testing, and the likelihood of reagent shortages, especially in resource-poor settings, we have developed a RT-qPCR assay that relies on an alternative to conventional viral reverse transcriptases, a thermostable reverse transcriptase / DNA polymerase (RTX)[1]. Here we show that RTX performs comparably to the other assays sanctioned by the CDC and validated in kit format. We demonstrate two modes of RTX use – (i) dye-based RT-qPCR assays that require only RTX polymerase, and (ii) TaqMan RT-qPCR assays that use a combination of RTX and Taq DNA polymerases (as the RTX exonuclease does not degrade a TaqMan probe). We also provide straightforward recipes for the purification of this alternative reagent. We anticipate that in low resource or point-of-need settings researchers could obtain the available constructs from Addgene or our lab and begin to develop their own assays, within whatever regulatory framework exists for them.

We lay out protocols for dye-based and TaqMan probe-based assays, in order to best compare with 'gold standard' reagents. These protocols should form the basis of further modifications that can simplify the assay to the use of overexpressing cells themselves as reagents.

Developing dye-based and TaqMan probe-based RT-qPCR assays with RTX

MATERIALS

- 10X RTX buffer: 600 mM Tris-HCl, 250 mM $(NH_4)_2SO_4$, 100 mM KCl, 20 mM $MgSO_4$, pH 8.4 @25°C
- 10X ThermoPol buffer (New England Biolabs): 200 mM Tris-HCl, 100 mM $(NH_4)_2SO_4$, 100 mM KCl, 20 mM $MgSO_4$, 1% Triton® X-100, pH 8.8 @25°C
- 6.7 µM Forward PCR primer[a]
- 6.7 µM Reverse PCR primer[a]
- 1.7 µM TaqMan probe[a]

bioRxiv preprint doi: https://doi.org/10.1101/2020.03.29.013342; this version posted April 9, 2020. The copyright holder for this preprint (which was not certified by peer review) is the author/funder, who has granted bioRxiv a license to display the preprint in perpetuity. It is made available under aCC-BY-NC-ND 4.0 International license.

- 20X EvaGreen solution
- 4 mM deoxyribonucleotides (dNTP)
- 5M Betaine
- 20 U/µL SUPERase.In RNase inhibitor
- 5 U/µL Taq DNA polymerase
- 0.2 mg/ml RTX polymerase[b]
- Nuclease-free water
- qPCR tubes or plates[c]
- Real-time PCR machine[c]
- Cold-block or ice
- Barrier tips

[a]Individual primer and probe stocks or pre-made primer-probe mixes for CDC N1, N2 and N3 assays (**Table 1**) available from Integrated DNA Technologies may be used.

[b]RTX polymerase with proofreading capability (RTX), and RTX polymerase without proofreading capability (RTX Exo-) have been compared.

[c]LightCycler96 real-time PCR machine and 96-well plates with optical plastic film cover designed for use with LightCycler platform were used for these experiments.

Table 1. CDC TaqMan qRT-PCR primers and probes for SARS-CoV-2 (adapted from https://www.cdc.gov/coronavirus/2019-ncov/lab/rt-pcr-panel-primer-probes.html).

Name	Description	Sequence[a]
2019-nCoV_N1-F	2019-nCoV_N1 Forward Primer	5'-GAC CCC AAA ATC AGC GAA AT-3'
2019-nCoV_N1-R	2019-nCoV_N1 Reverse Primer	5'-TCT GGT TAC TGC CAG TTG AAT CTG-3'
2019-nCoV_N1-P	2019-nCoV_N1 Probe	5'-FAM-ACC CCG CAT TAC GTT TGG ACC-BHQ1-3'
2019-nCoV_N2-F	2019-nCoV_N2 Forward Primer	5'-TTA CAA ACA TTG GCC GCA AA-3'
2019-nCoV_N2-R	2019-nCoV_N2 Reverse Primer	5'-GCG CGA CAT TCC GAA GAA-3'
2019-nCoV_N2-P	2019-nCoV_N2 Probe	5'-FAM-ACA ATT TGC CCC CAG CGC TTC AG-BHQ1-3'
2019-nCoV_N3-F	2019-nCoV_N3 Forward Primer	5'-GGG AGC CTT GAA TAC ACC AAA A-3'
2019-nCoV_N3-R	2019-nCoV_N3 Reverse Primer	5'-TGT AGC ACG ATT GCA TTG-3'
2019-nCoV_N3-P	2019-nCoV_N3 Probe	5'-FAM-AYC ACA TTG GCA CCC GCA ATC CTG-BHQ1-3'

[a]FAM: 6-carboxyfluorescein; BHQ-1: Black Hole Quencher 1

RESULTS

Dye-based RT-qPCR reaction set up using only RTX DNA polymerase

EvaGreen dye-containing RT-qPCR reaction set up shown in **Table 2** was used for assembling CDC SARS-CoV-2 N1, N2, and N3 assays. The three assays target three different regions within the

bioRxiv preprint doi: https://doi.org/10.1101/2020.03.29.013342; this version posted April 9, 2020. The copyright holder for this preprint (which was not certified by peer review) is the author/funder, who has granted bioRxiv a license to display the preprint in perpetuity. It is made available under aCC-BY-NC-ND 4.0 International license.

nucleocapsid phosphoprotein (N) gene near the 3'-end of the ~30 kb viral genome. In particular, N1 primers (**Table 1**) amplify a 71 nt long region from position 28287 to 28358 of the genome (GenBank Accession No. MN985325.1). The N2 primers produce a 66 bp amplicon from the genomic position 29164 to 29230. Meanwhile, the N3 primers amplify a 71 nt long region from genomic position 28681 to 28752. All reaction mixes were assembled on a cold-block and directly transferred to a real-time PCR machine programmed to cycle through the steps depicted in **Table 3**. Melt curve analysis was included after PCR amplification in order to distinguish target amplicons from spurious products.

Table 2. EvaGreen RT-qPCR reaction mix using only RTX DNA polymerase

	Volume (µL)	Final concentration
RNA sample	5	
6.7 µM Forward PCR primer	1.5	500 nM
6.7 µM Reverse PCR primer	1.5	500 nM
20X EvaGreen	1.25	1X
10X RTX buffer	2.5	1X
4 mM dNTP	2.5	400 µM
20 U/µL SUPERase.In RNase inhibitor	1	0.8 U/µL
RTX or RTX Exo- 0.2mg/ml	0.5	4 ng/µL
5M betaine	2.5	0.5M
Water	6.75	
Total reaction volume	25	

Table 3. RTX polymerase-based EvaGreen RT-qPCR cycling conditions

Step	Temperature	Duration	Signal acquisition
1[a]	60 °C	30 min	None
2[a]	95 °C	10 min	None
55 cycles of Steps 3 and 4			
3	95 °C	15 sec	None
4[b]	55 °C	30 sec	Single
Melt curve analysis in Steps 5, 6, and 7			
5	95 °C	10 sec	None
6	65 °C	60 sec	None
7	97 °C	1 sec	Continuous[c]

[a]Assay time may be reduced by shortening reverse transcription step (Step 1) to 15 min and the following denaturation step (Step 2) to 2 min.

[b]Signal acquisition occurs in the FAM (fluorescein) channel during step 4.

bioRxiv preprint doi: https://doi.org/10.1101/2020.03.29.013342; this version posted April 9, 2020. The copyright holder for this preprint (which was not certified by peer review) is the author/funder, who has granted bioRxiv a license to display the preprint in perpetuity. It is made available under aCC-BY-NC-ND 4.0 International license.

[c]20 measurements/°C temperature change, at a ramp rate of 0.05 °C/sec

Representative results of SARS-CoV-2 RT-qPCR tests performed using synthetic RNA templates and only RTX or RTX Exo- DNA polymerases are depicted in **Figures 1 and 2**.

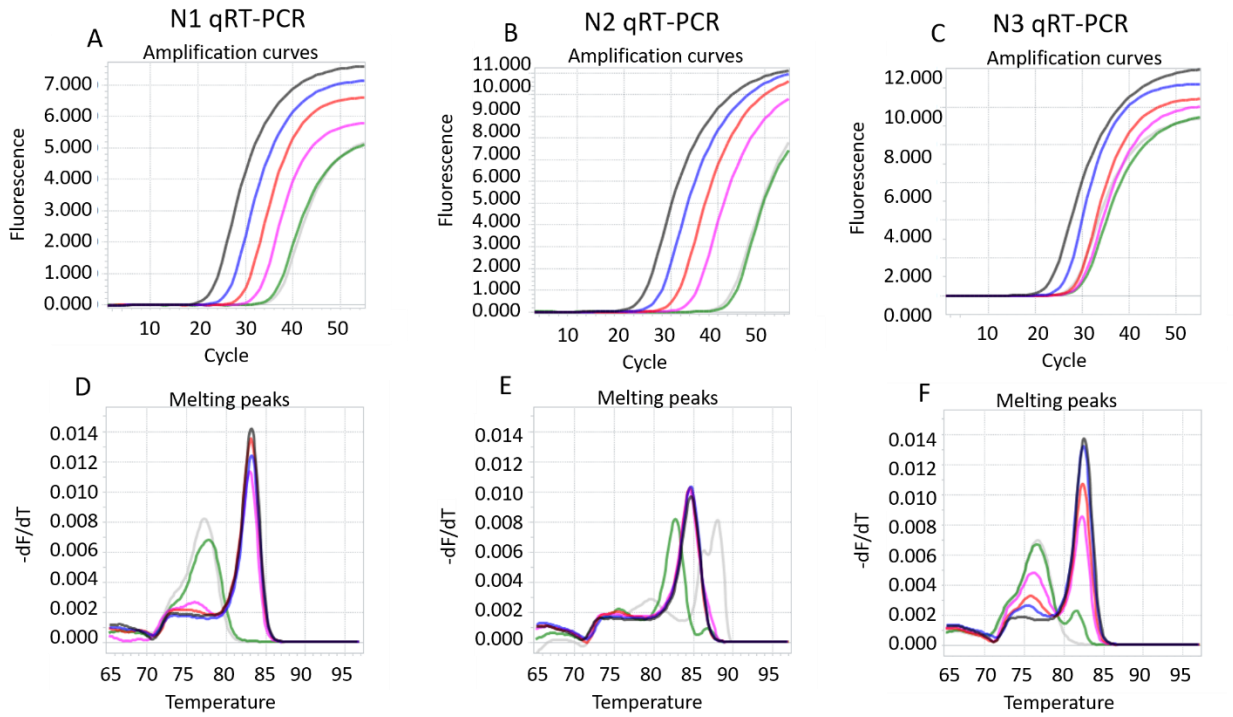

N1 qRT-PCR	Average Cq
100,000 nCoV-2019 N RNA	19.19
10,000 nCoV-2019 N RNA	22.87
1,000 nCoV-2019 N RNA	26.48
100 nCoV-2019 N RNA	29.52
100,000 MERS N RNA	33.19
No template	34.13

N2 qRT-PCR	Average Cq
100,000 nCoV-2019 N RNA	19.35
10,000 nCoV-2019 N RNA	22.87
1,000 nCoV-2019 N RNA	26.79
100 nCoV-2019 N RNA	30.30
100,000 MERS N RNA	38.69
No template	37.67

N3 qRT-PCR	Average Cq
100,000 nCoV-2019 N RNA	18.40
10,000 nCoV-2019 N RNA	22.08
1,000 nCoV-2019 N RNA	25.03
100 nCoV-2019 N RNA	26.65
100,000 MERS N RNA	27.85
No template	25.11

Figure 1. CDC SARS-CoV-2 N1, N2, and N3 RT-qPCR assays performed using indicated copies of synthetic RNA and RTX DNA polymerase. Panels A, B, and C depict N1, N2, and N3 assays measured in real-time using EvaGreen dye. Amplification curves from reactions containing 100,000 (black traces), 10,000 (blue traces), 1,000 (red traces), and 100 (pink traces) copies of SARS-CoV-2 synthetic N RNA are depicted. Negative control reactions either contained no templates (gray traces) or contained 100,000 copies of synthetic N RNA from MERS-CoV (green traces). Panels D, E, and F depict melting peaks of amplicons determined using the 'Tm calling' analysis in the LightCycler96 software. Average Cq values of all assays are tabulated.

bioRxiv preprint doi: https://doi.org/10.1101/2020.03.29.013342; this version posted April 9, 2020. The copyright holder for this preprint (which was not certified by peer review) is the author/funder, who has granted bioRxiv a license to display the preprint in perpetuity. It is made available under aCC-BY-NC-ND 4.0 International license.

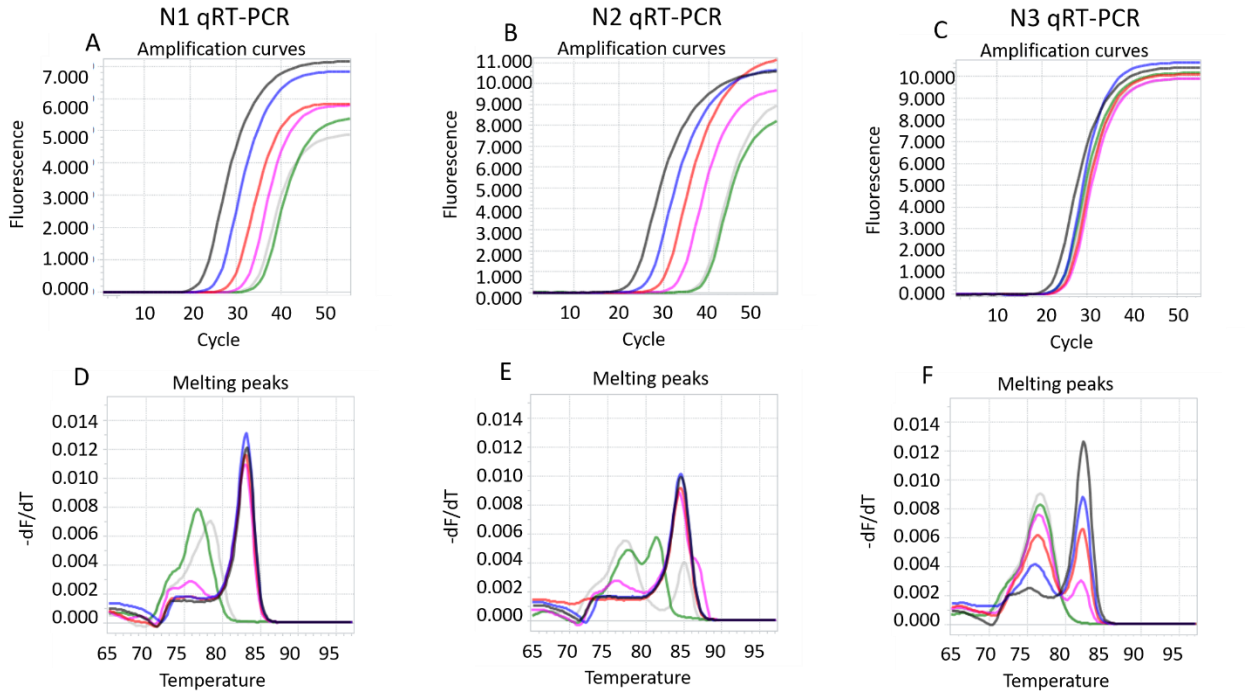

N1 qRT-PCR	Average Cq
100,000 nCoV-2019 N RNA	19.39
10,000 nCoV-2019 N RNA	23.065
1,000 nCoV-2019 N RNA	26.53
100 nCoV-2019 N RNA	29.65
100,000 MERS N RNA	32.36
No template	32.23

N2 qRT-PCR	Average Cq
100,000 nCoV-2019 N RNA	18.945
10,000 nCoV-2019 N RNA	22.56
1,000 nCoV-2019 N RNA	25.95
100 nCoV-2019 N RNA	29.56
100,000 MERS N RNA	34.86
No template	34.45

N3 qRT-PCR	Average Cq
100,000 nCoV-2019 N RNA	18.945
10,000 nCoV-2019 N RNA	21.47
1,000 nCoV-2019 N RNA	22.32
100 nCoV-2019 N RNA	22.52
100,000 MERS N RNA	21.86
No template	21.93

Figure 2. CDC SARS-CoV-2 N1, N2, and N3 RT-qPCR assays performed using indicated copies of synthetic RNA and RTX Exo- DNA polymerase. Panels A, B, and C depict N1, N2, and N3 assays measured in real-time using EvaGreen dye. Amplification curves from reactions containing 100,000 (black traces), 10,000 (blue traces), 1,000 (red traces), and 100 (pink traces) copies of SARS-CoV-2 synthetic N RNA are depicted. Negative control reactions either contained no templates (gray traces) or contained 100,000 copies of synthetic N RNA from MERS-CoV (green traces). Panels D, E, and F depict melting peaks of amplicons determined using the 'Tm calling' analysis in the LightCycler96 software. Average Cq values of all assays are tabulated.

These results demonstrate that RTX DNA polymerase alone, with or without proofreading capability, can support dye-based RT-qPCR analyses. In our hands the full-length RTX DNA polymerase was slightly better than the Exo- version, especially in the N3 assay.

RTX polymerase-based TaqMan qRT-PCR reaction set up

In order to perform TaqMan RT-qPCR we developed a one-pot two enzyme system comprising RTX and Taq DNA polymerases. TaqMan qRT-PCR reaction set up shown in **Table 4** was used for assembling CDC SARS-CoV-2 N1, N2, and N3 assays using either RTX buffer or ThermoPol buffer. Control reactions lacking RTX polymerase were set up using the same recipe except RTX was

bioRxiv preprint doi: https://doi.org/10.1101/2020.03.29.013342; this version posted April 9, 2020. The copyright holder for this preprint (which was not certified by peer review) is the author/funder, who has granted bioRxiv a license to display the preprint in perpetuity. It is made available under aCC-BY-NC-ND 4.0 International license.

replaced with water. All reaction mixes were assembled on a cold-block and directly transferred to a real-time PCR machine programmed to cycle through the steps depicted in **Table 5**.

Table 4. RTX polymerase-based TaqMan qRT-PCR reaction mix

	Volume (µL)	Final concentration
RNA sample	5	
6.7 µM Forward PCR primer	1.5	500 nM
6.7 µM Reverse PCR primer	1.5	500 nM
1.7 µM TaqMan probe	1.5	125 nM
10X Assay buffer[a]	2.5	1X
4 mM dNTP	2.5	400 µM
20 U/µL SUPERase.In RNase inhibitor	1	0.8 U/µL
5 U/ µL Taq DNA polymerase	0.5	0.1 U/µL
RTX or RTX Exo- 0.2mg/ml or water	0.5	4 ng/µL
5M betaine	2.5	0.5M
Water	6	
Total reaction volume	25	

[a] Assay buffer: Duplicate TaqMan RT-qPCR reactions were performed either in 1X ThermoPol buffer or in 1X RTX buffer as indicated.

Table 5. RTX polymerase-based TaqMan qRT-PCR cycling conditions

Step 1[a]	60 °C	30 min
Step 2[a]	95 °C	10 min
55 cycles of Steps 3 and 4		
Step 3	95 °C	15 sec
Step 4[b]	55 °C	30 sec

[a]Assay time may be reduced by shortening reverse transcription step (Step 1) to 15 min and the following denaturation step (Step 2) to 2 min.

[b]Signal acquisition occurs in the FAM (fluorescein) channel during step 4.

Representative results of RTX polymerase-based SARS-CoV-2 TaqMan qRT-PCR tests performed using synthetic RNA templates are depicted in **Figures 3 and 4**. Both RTX and RTX Exo- when combined with Taq DNA polymerase were able to support one-pot TaqMan RT-qPCR assays for all three CDC SARS-CoV-2 assays. Under both buffer conditions tested, 1X ThermoPol versus 1X RTX buffer, RTX polymerase yielded more consistent amplification curves for all three CDC assays compared to RTX Exo- polymerase.

bioRxiv preprint doi: https://doi.org/10.1101/2020.03.29.013342; this version posted April 9, 2020. The copyright holder for this preprint (which was not certified by peer review) is the author/funder, who has granted bioRxiv a license to display the preprint in perpetuity. It is made available under aCC-BY-NC-ND 4.0 International license.

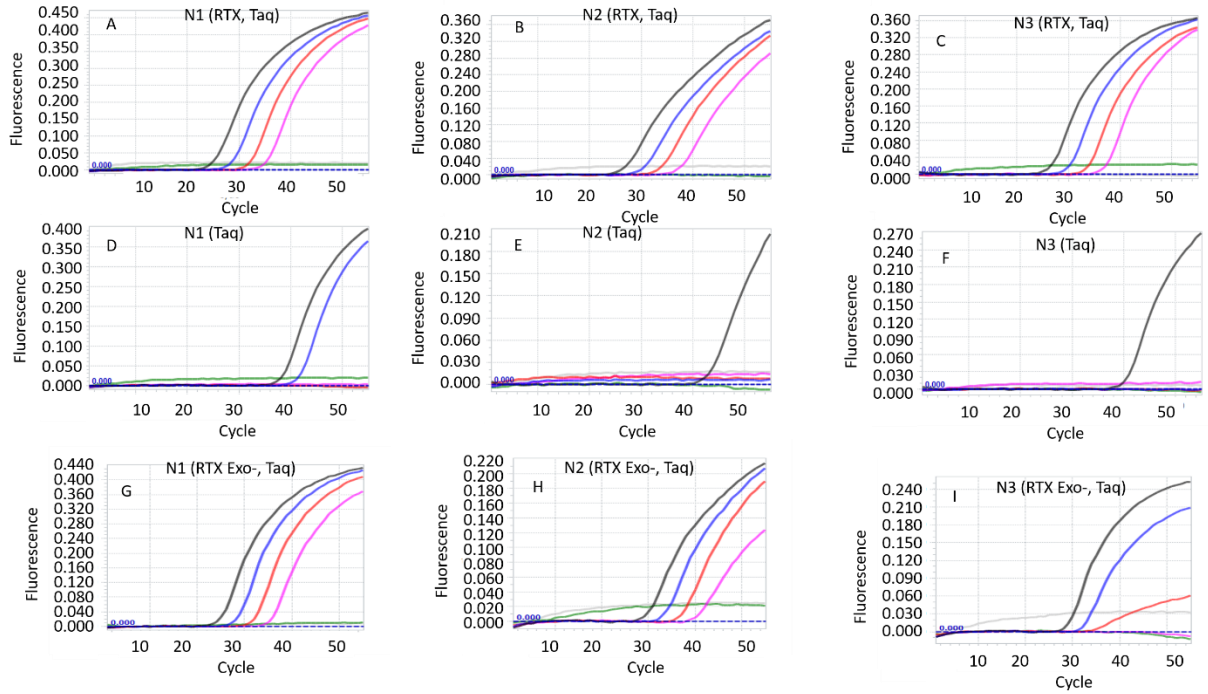

N1 qRT-PCR in ThermoPol	RTX	Taq	RTX Exo-
100,000 nCoV-2019 N RNA	26.19	39.48	26.15
10,000 nCoV-2019 N RNA	29.71	42.74	29.71
1,000 nCoV-2019 N RNA	33.21	--	33.33
100 nCoV-2019 N RNA	36.29	--	36.99
100,000 MERS N RNA	--	--	--
No template	--	--	--

N2 qRT-PCR in ThermoPol	RTX	Taq	RTX Exo-
100,000 nCoV-2019 N RNA	28.81	45.56	--
10,000 nCoV-2019 N RNA	32.47	--	36.63
1,000 nCoV-2019 N RNA	35.78	--	40.48
100 nCoV-2019 N RNA	39.53	--	--
100,000 MERS N RNA	--	--	--
No template	--	--	--

N3 qRT-PCR in ThermoPol	RTX	Taq	RTX Exo-
100,000 nCoV-2019 N RNA	28.03	42.16	--
10,000 nCoV-2019 N RNA	31.53	--	--
1,000 nCoV-2019 N RNA	35.16	--	--
100 nCoV-2019 N RNA	38.51	--	--
100,000 MERS N RNA	--	--	--
No template	--	--	--

Figure 3. CDC SARS-CoV-2 N1, N2, and N3 TaqMan RT-qPCR assays performed in 1X ThermoPol buffer using indicated copies of synthetic RNA and RTX or RTX Exo- and Taq DNA polymerases. Panels A, B, and C depict TaqMan assays containing both RTX and Taq DNA polymerases. Panels D, E, and F depict TaqMan assays containing only Taq DNA polymerase. Panels G, H, and I depict TaqMan assays containing RTX Exo- and Taq DNA polymerases. Amplification curves from reactions containing 100,000 (black traces), 10,000 (blue traces), 1,000 (red traces), and 100 (pink traces) copies of SARS-CoV-2 synthetic N RNA are depicted. Negative control reactions either contained no templates (gray traces) or contained 100,000 copies of synthetic N RNA from MERS-CoV (green traces). Cq values of all assays are tabulated.

bioRxiv preprint doi: https://doi.org/10.1101/2020.03.29.013342; this version posted April 9, 2020. The copyright holder for this preprint (which was not certified by peer review) is the author/funder, who has granted bioRxiv a license to display the preprint in perpetuity. It is made available under aCC-BY-NC-ND 4.0 International license.

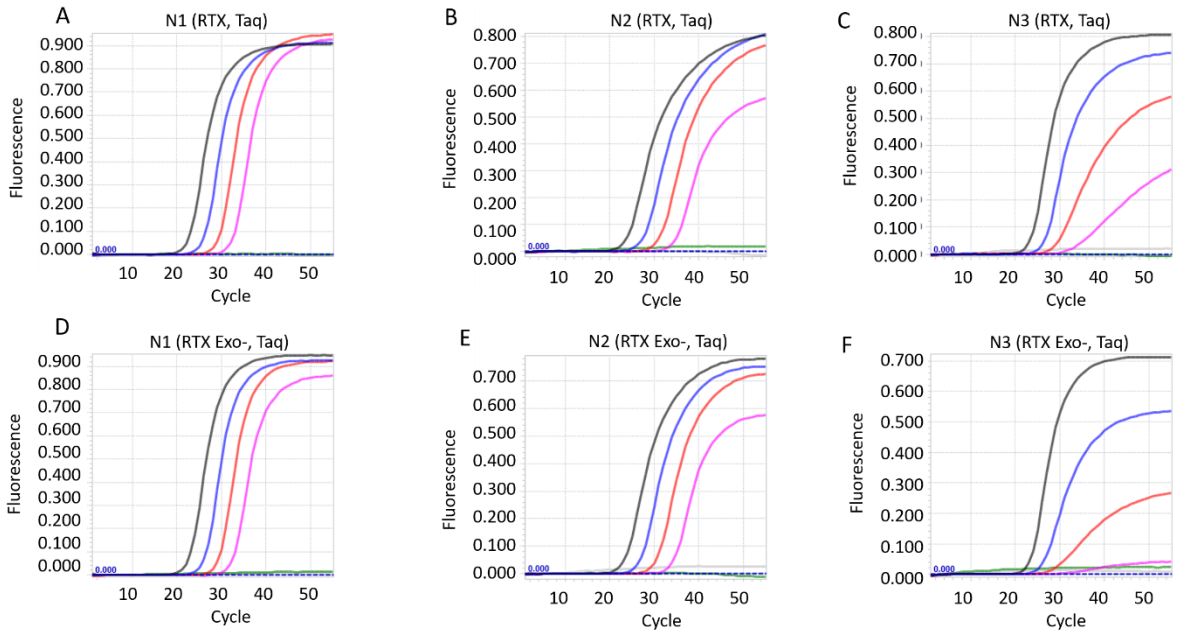

N1 qRT-PCR in RTX buffer	RTX	RTX Exo-
100,000 nCoV-2019 N RNA	22.18	22.18
10,000 nCoV-2019 N RNA	25.54	25.64
1,000 nCoV-2019 N RNA	28.88	28.92
100 nCoV-2019 N RNA	32.06	32.14
100,000 MERS N RNA	--	--
No template	--	--

N2 qRT-PCR in RTX buffer	RTX	RTX Exo-
100,000 nCoV-2019 N RNA	23.77	23.27
10,000 nCoV-2019 N RNA	27.46	26.81
1,000 nCoV-2019 N RNA	31.09	30.43
100 nCoV-2019 N RNA	34.97	34.36
100,000 MERS N RNA	--	--
No template	--	--

N3 qRT-PCR in RTX buffer	RTX	RTX Exo-
100,000 nCoV-2019 N RNA	23.28	23.43
10,000 nCoV-2019 N RNA	26.55	26.63
1,000 nCoV-2019 N RNA	29.77	--
100 nCoV-2019 N RNA	35.44	--
100,000 MERS N RNA	--	--
No template	--	--

Figure 4. CDC SARS-CoV-2 N1, N2, and N3 TaqMan RT-qPCR assays performed in 1X RTX buffer using indicated copies of synthetic RNA and RTX or RTX Exo- and Taq DNA polymerases. Panels A, B, and C depict TaqMan assays containing RTX and Taq DNA polymerases. Panels D, E, and F depict TaqMan assays containing RTX Exo- and Taq DNA polymerases. Amplification curves from reactions containing 100,000 (black traces), 10,000 (blue traces), 1,000 (red traces), and 100 (pink traces) copies of SARS-CoV-2 synthetic N RNA are depicted. Negative control reactions either contained no templates (gray traces) or contained 100,000 copies of synthetic N RNA from MERS-CoV (green traces). Cq values of all assays are tabulated.

To compare the RTX-based TaqMan qRT-PCR with qRT-PCR performed using commercial master mix, duplicate reactions (**Table 6**) were set up using TaqPath™ 1-Step RT-qPCR Master Mix, CG (Thermo Fisher Scientific, Waltham, MA, USA). All reactions were assembled on cold block and then incubated at room temperature (25 °C benchtop) for 2 min prior to being loaded on a real-time PCR machine set to cycle through the steps indicated in **Table 7**.

bioRxiv preprint doi: https://doi.org/10.1101/2020.03.29.013342; this version posted April 9, 2020. The copyright holder for this preprint (which was not certified by peer review) is the author/funder, who has granted bioRxiv a license to display the preprint in perpetuity. It is made available under aCC-BY-NC-ND 4.0 International license.

Table 6. CDC N1, N2, N3 TaqMan qRT-PCR assay set up using commercial qRT-PCR master mix

	Volume (µL)
RNA sample	5
6.7 µM Forward PCR primer	1.5
6.7 µM Reverse PCR primer	1.5
1.7 µM TaqMan probe	1.5
4X TaqPath™ master mix	5
Water	5.5
Total reaction volume	20

Table 7. TaqPath™ TaqMan qRT-PCR cycling conditions

Step 1	50 °C	15 min
Step 2	95 °C	2 min
45 cycles of Steps 3 and 4		
Step 3	95 °C	3 sec
Step 4	55 °C	30 sec

Figure 5 depicts typical results from CDC N1, N2, and N3 TaqMan qRT-PCR reactions performed using synthetic RNA and TaqPath™ commercial qRT-PCR mastermix.

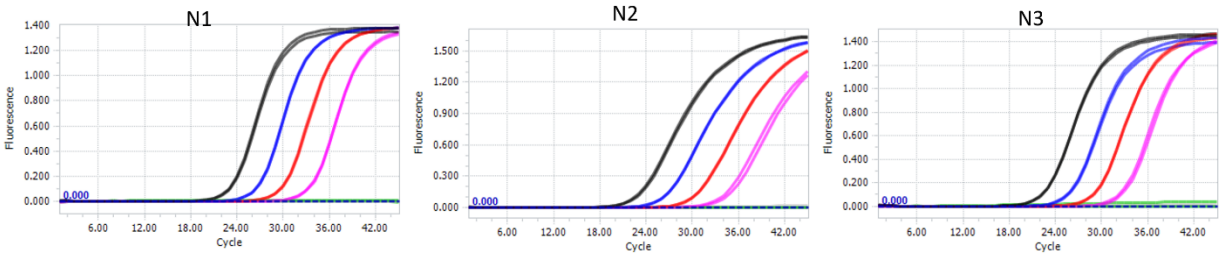

N1 qRT-PCR	TaqPath
100,000 nCoV-2019 N RNA	22.02
10,000 nCoV-2019 N RNA	25.55
1,000 nCoV-2019 N RNA	28.79
100 nCoV-2019 N RNA	32.21
100,000 MERS N RNA	--
No template	--

N2 qRT-PCR	TaqPath
100,000 nCoV-2019 N RNA	21.57
10,000 nCoV-2019 N RNA	25.16
1,000 nCoV-2019 N RNA	28.90
100 nCoV-2019 N RNA	32.58
100,000 MERS N RNA	--
No template	--

N3 qRT-PCR	TaqPath
100,000 nCoV-2019 N RNA	21.20
10,000 nCoV-2019 N RNA	24.56
1,000 nCoV-2019 N RNA	27.98
100 nCoV-2019 N RNA	31.59
100,000 MERS N RNA	--
No template	--

Figure 5. CDC SARS-CoV-2 N1, N2, and N3 TaqMan qRT-PCR assays performed using indicated copies of synthetic RNA and TaqPath™ commercial qRT-PCR mastermix. Amplification curves from reactions containing 100,000 (black traces), 10,000 (blue traces), 1,000 (red traces), and 100 (pink traces) copies of SARS-CoV-2 synthetic N RNA are depicted. Negative control reactions either contained no templates (gray traces) or contained 100,000 copies of synthetic N RNA from MERS-CoV (green traces). Cq values of all assays are tabulated.

bioRxiv preprint doi: https://doi.org/10.1101/2020.03.29.013342; this version posted April 9, 2020. The copyright holder for this preprint (which was not certified by peer review) is the author/funder, who has granted bioRxiv a license to display the preprint in perpetuity. It is made available under aCC-BY-NC-ND 4.0 International license.

The results with either a viral RT (in TaqPath™ commercial mastermix) or RTX are summarized in **Table 8**. As can be seen, RTX-based TaqMan assays are of comparable sensitivity and specificity to the gold standard TaqPath assay. While all three RTX-based TaqMan assays performed in ThermoPol buffer consistently yielded Cq values, these were somewhat delayed compared to Cq values obtained with the commercial TaqPath™ Master Mix. In contrast, RTX-based TaqMan assays when executed in RTX buffer yielded Cq values that were closer to Cq values obtained with the commercial mastermix.

Table 8. Comparison of Cq values of RTX-based and TaqPath-based SARS-CoV-2 TaqMan qRT-PCR assays

N1 qRT-PCR	RTX+Taq in ThermoPol	RTX+Taq in RTX buffer	TaqPath™
100,000 nCoV-2019 N RNA	26.19	22.18	22.02
10,000 nCoV-2019 N RNA	29.71	25.54	25.55
1,000 nCoV-2019 N RNA	33.21	28.88	28.79
100 nCoV-2019 N RNA	36.29	32.06	32.21
100,000 MERS N RNA	--		--
No template	--		--

N2 qRT-PCR	RTX+Taq in ThermoPol	RTX+Taq in RTX buffer	TaqPath™
100,000 nCoV-2019 N RNA	28.81	23.77	21.57
10,000 nCoV-2019 N RNA	32.47	27.46	25.16
1,000 nCoV-2019 N RNA	35.78	31.09	28.90
100 nCoV-2019 N RNA	39.53	34.97	32.58
100,000 MERS N RNA	--		--
No template	--		--

N3 qRT-PCR	RTX+Taq in ThermoPol	RTX+Taq in RTX buffer	TaqPath™
100,000 nCoV-2019 N RNA	28.03	23.28	21.20
10,000 nCoV-2019 N RNA	31.53	26.55	24.56
1,000 nCoV-2019 N RNA	35.16	29.77	27.98
100 nCoV-2019 N RNA	38.51	35.44	31.59
100,000 MERS N RNA	--		--
No template	--		--

<u>Summary of assay performance</u>

Overall, RTX performs well either as a single enzyme for RT-qPCR with intercalating dyes, such as EvaGreen, or as the RT component of a TaqMan based assay. At the lowest RNA concentrations examined (100 copies), the gold standard TaqPath assay general gave a signal at a Cq value of ca. 32. The more robust full-length RTX on its own actually performed slightly better, with C_q values typically from 29-30 (although the N3 primer set gives higher signal and higher background). When used as a substitute for a viral RT, RTX is slightly less sensitive overall, with Cq values typically from 32-35.

bioRxiv preprint doi: https://doi.org/10.1101/2020.03.29.013342; this version posted April 9, 2020. The copyright holder for this preprint (which was not certified by peer review) is the author/funder, who has granted bioRxiv a license to display the preprint in perpetuity. It is made available under aCC-BY-NC-ND 4.0 International license.

Purification of RTX

For sites wishing to produce their own RTX, the following protocol can be used.

Resuspension Buffer	• 50 mM Phosphate Buffer, pH 7.5 • 300 mM NaCl • 20 mM imidazole • 0.1% Igepal CO-630 (non-toxic Non-idet P40 equivalent) • 5 mM MgSO4
Equilibration Buffer	• 50 mM Phosphate Buffer, pH 7.5 • 300 mM NaCl • 20 mM imidazole
Lysis Buffer	• 30 mL **Resuspension Buffer** + • 1x EDTA-free protease inhibitor tablet + • 30-60 mg HEW Lysozyme
Wash Buffer	• 50 mM Phosphate Buffer, pH 7.5 • 300 mM NaCl • 50 mM imidazole
Elution Buffer	• 50 mM Phosphate Buffer, pH 7.5 • 300 mM NaCl • 250 mM imidazole
Heparin Buffer A	• 40 mM Tris-HCl, pH 7.5 • 100 mM NaCl • 0.1% Igepal CO-630 (non-toxic Non-idet P40 equivalent)
Heparin Buffer B	• 40 mM Tris-HCl, pH 7.5 • 2 M NaCl • 0.1% Igepal CO-630 (non-toxic Non-idet P40 equivalent)

Table 7. Buffers for RTX purification

Ni-NTA Dialysis Buffer (2x 2 L)	• 40 mM Tris-HCl, pH 7.5 • 100 mM NaCl • 10 mM beta-mercapto ethanol (BME) or 1 mM DTT • 0.1% Igepal CO-630 (non-toxic Non-idet P40 equivalent)
Heparin Dialysis Buffer (2 L)	• 50 mM Tris-HCl, pH 8.0 • 50 mM KCl • 0.1% Tween-20 • 0.1% Igepal CO-630 (non-toxic Non-idet P40 equivalent)
Final Dialysis Buffer (1 L)	• 50% Glycerol • 50 mM Tris-HCl, pH 8.0

bioRxiv preprint doi: https://doi.org/10.1101/2020.03.29.013342; this version posted April 9, 2020. The copyright holder for this preprint (which was not certified by peer review) is the author/funder, who has granted bioRxiv a license to display the preprint in perpetuity. It is made available under aCC-BY-NC-ND 4.0 International license.

	• 50 mM KCl • 0.1% Tween-20 • 0.1% Igepal CO-630 (non-toxic Non-idet P40 equivalent)

Table 8. Buffers for dialysis of RTX

In brief, a T7-based *E. coli* expression strain such as BL21(DE3) was transformed with a RTX expression plasmid that contained an carboxyl terminal six histidine tag for purification. On the next day, an individual transformant colony was picked into desired media with appropriate antibiotics (e.g. ampicillin) and 1-2% glucose. This starter culture was grown overnight in shaking incubator at 37˚C.

On day three, 1 L Superior Broth™ (Athena Enzyme Systems™) or other rich media with appropriate antibiotics in a 4 L Erlenmeyer flask was inoculated with 250-350 µL of the overnight starter culture. Incubate at 37˚C, 250 rpm until the culture reaches OD_{600} of 0.4-0.7 (0.5-0.6 is ideal). When desired OD_{600} is reached, place flask(s) in 4˚C cold room for 30-45 min and set shaking incubator to 18˚C. Following cold incubation, induce expression of RTX by adding 1 mL of 1 M IPTG to each 1 L of culture. Place flask(s) in the 18˚C shaking incubator for 16-18 hours.

Following overnight expression, cells were harvested by centrifuging cultures at 4˚C, 5000 xg for 20 min. On ice, resuspend cell pellet in 30 mL cold **Lysis Buffer**. Transfer the resuspended cell pellet to a small 50 mL beaker with clean stir bar and place securely in an ice bath. With moderate stirring, sonicate the sample using 40% amplitude and 1 sec ON / 4 sec OFF for 4 min total sonication time. Centrifuge the resulting lysate at 4˚C, 35,000 xg for 30 min. Carefully transfer the supernatant to a clean ultracentrifugation tube, shake in thermomixer at 400 rpm, 85˚C for 10 min, and then place on ice for 10 min. Centrifuged the heat-treated lysate at 4˚C, 35,000 xg for 30 min. Carefully transfer the supernatant to a clean tube and filter the clarified lysate using a 0.2 µm filter.

Perform IMAC column purification in a cold room or allow gravity flow to occur in a refrigerator. Prepare Ni-NTA agarose columns with final column volume (CV) of 1 mL. Apply the clarified lysate from 1 L of expressed culture to a previously equilibrated column and collect the flow-through. Wash column with 20 CV **Equilibration Buffer** and collect the flow-through. Wash column with 5 CV **Wash Buffer** and collect flow-through. Elute RTX from column with 5 mL **Elution Buffer** and transfer to a dialysis cassette with appropriate molecular weight cut-off. Dialyze eluate into 2 L of **Ni-NTA Dialysis Buffer** for 3-4 hours at 4˚C. Then dialyze eluate into a second 2 L of **Ni-NTA Dialysis Buffer** overnight at 4˚C.

Dialyzed eluate was then passed over an equilibrated 5 mL heparin column (HiTrap™ Heparin HP) and eluted along a sodium chloride gradient (100 mM to 2 M NaCl). The peak corresponding to RTX or its variants could be expected between 40-60% Buffer B. RTX fractions were collected, pooled, and dialyzed into 2 L **Heparin Dialysis Buffer** for 3-4 hours. Then dialysis cassettes were transferred into 2 L **Final Dialysis Buffer** overnight where it is expected that the protein sample

bioRxiv preprint doi: https://doi.org/10.1101/2020.03.29.013342; this version posted April 9, 2020. The copyright holder for this preprint (which was not certified by peer review) is the author/funder, who has granted bioRxiv a license to display the preprint in perpetuity. It is made available under aCC-BY-NC-ND 4.0 International license.

volume will decrease significantly. Following the final dialysis, protein sample was recovered and protein concentration was determined before storing at -20˚C.

A similar protocol should work for Taq and other thermostable polymerases, but may require different dialysis and storage buffers.

Summary and opportunities for distribution

By obtaining a RTX expression vector and purifying the thermostable reverse transcriptase it should prove possible to carry out RT-qPCR reactions with a sensitivity similar to that already observed for approved kits, with few or no false positive results. The sequence information for plasmids for RTX [pET_RTX-6xHis] and its exonuclease deficient variant, RTX(exo-) [pET_RTX(exo-)-6xHis], bearing a C-terminal 6xHis tags can be found in the **Supplemental Information**. These plasmids will be uploaded to Addgene in short order, or can be obtained by directly contacting the Ellington lab, via a.maranhao@utexas.edu. The Board of Regents of The University of Texas has licensed IP covering RTX to Promega Corporation.

Acknowledgements: We acknowledge the extraordinary contributions of the Schoggins lab in making synthetic RNA available on short notice for these assays.

bioRxiv preprint doi: https://doi.org/10.1101/2020.03.29.013342; this version posted April 9, 2020. The copyright holder for this preprint (which was not certified by peer review) is the author/funder, who has granted bioRxiv a license to display the preprint in perpetuity. It is made available under aCC-BY-NC-ND 4.0 International license.

Supporting Information

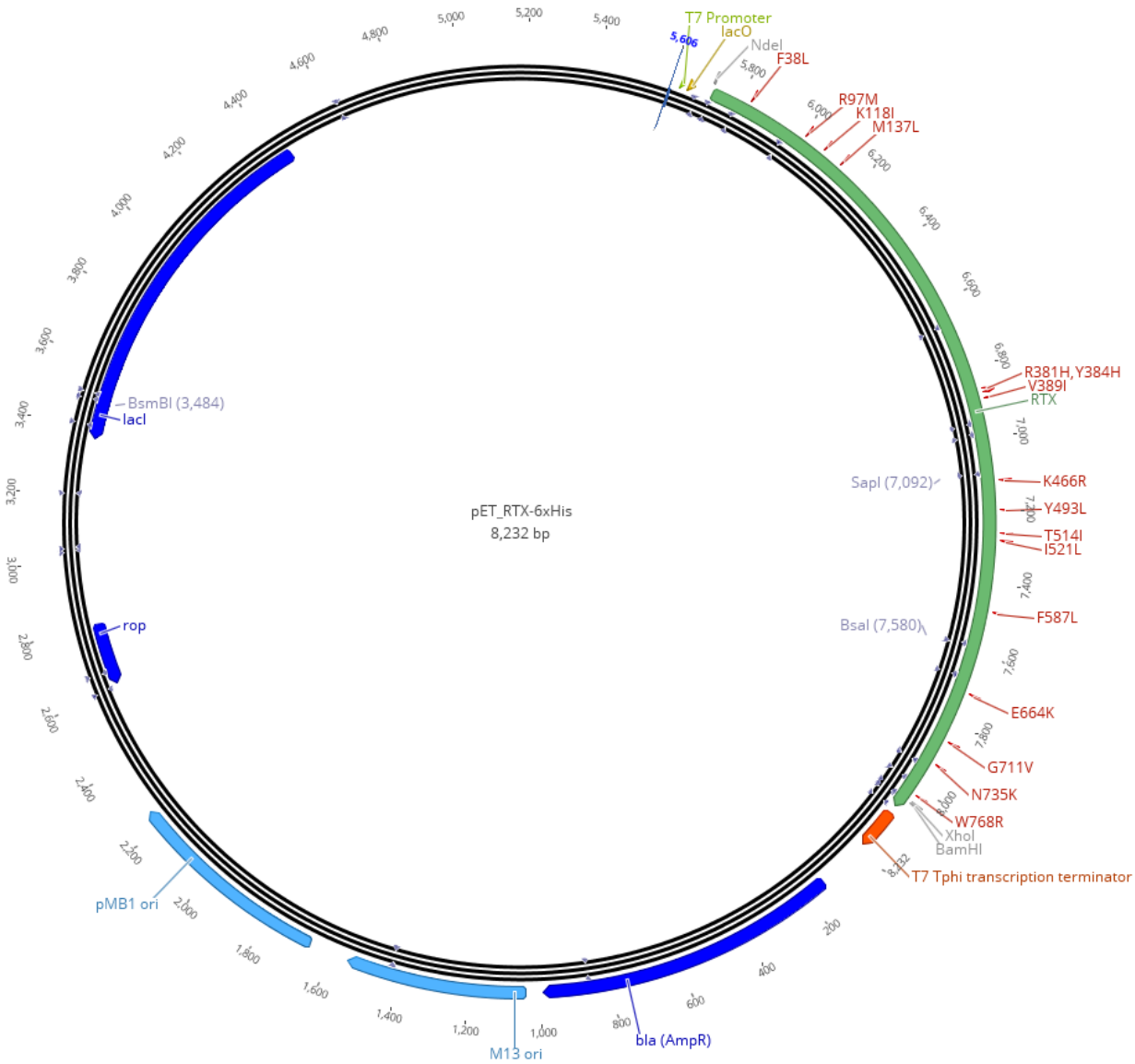

Figure S1. Plasmid map of pET_RTX-6xHis

```
LOCUS       pET_RTX-6xHis          8232 bp    DNA     circular UNA 26-MAR-2020
DEFINITION  A new nucleotide sequence entered manually.
ACCESSION   urn.local...f-bq4nr1q
VERSION     urn.local...f-bq4nr1q
KEYWORDS    .
SOURCE
  ORGANISM
            .
FEATURES             Location/Qualifiers
     gene            140..1000
```

bioRxiv preprint doi: https://doi.org/10.1101/2020.03.29.013342; this version posted April 9, 2020. The copyright holder for this preprint (which was not certified by peer review) is the author/funder, who has granted bioRxiv a license to display the preprint in perpetuity. It is made available under aCC-BY-NC-ND 4.0 International license.

```
                /created_by="User"
                /label="bla (AmpR)"
     rep_origin     1042..1555
                /created_by="User"
                /modified_by="User"
                /label="M13 ori"
     rep_origin     1666..2254
                /created_by="User"
                /modified_by="User"
                /label="pMB1 ori"
     gene           complement(2623..2814)
                /created_by="User"
                /label="rop"
     gene           complement(3371..4453)
                /created_by="User"
                /label="lacI"
     promoter       5637..5654
                /created_by="User"
                /label="T7 Promoter"
     operon         5656..5680
                /created_by="User"
                /label="lacO"
     misc_feature   5722..5727
                /created_by="User"
                /modified_by="User"
                /label="NdeI"
     CDS            5725..8085
                /created_by="User"
                /modified_by="User"
                /label="RTX"
     misc_difference 5836..5838
                /created_by="User"
                /label="F38L"
     misc_difference 6013..6015
                /created_by="User"
                /label="R97M"
     misc_difference 6076..6078
                /created_by="User"
                /modified_by="User"
                /label="K118I"
     misc_difference 6133..6135
                /created_by="User"
                /label="M137L"
     misc_difference 6865..6867
```

bioRxiv preprint doi: https://doi.org/10.1101/2020.03.29.013342; this version posted April 9, 2020. The copyright holder for this preprint (which was not certified by peer review) is the author/funder, who has granted bioRxiv a license to display the preprint in perpetuity. It is made available under aCC-BY-NC-ND 4.0 International license.

```
            /created_by="User"
            /label="R381H"
     misc_difference 6874..6876
            /created_by="User"
            /label="Y384H"
     misc_difference 6889..6891
            /created_by="User"
            /label="V389I"
     misc_difference 7120..7122
            /created_by="User"
            /label="K466R"
     misc_difference 7201..7203
            /created_by="User"
            /label="Y493L"
     misc_difference 7264..7266
            /created_by="User"
            /label="T514I"
     misc_difference 7285..7287
            /created_by="User"
            /label="I521L"
     misc_difference 7483..7485
            /created_by="User"
            /label="F587L"
     misc_difference 7714..7716
            /created_by="User"
            /label="E664K"
     misc_difference 7855..7857
            /created_by="User"
            /label="G711V"
     misc_difference 7927..7929
            /created_by="User"
            /label="N735K"
     misc_difference 8026..8028
            /created_by="User"
            /label="W768R"
     misc_feature    8047..8052
            /created_by="User"
            /label="XhoI"
     misc_feature    8053..8058
            /created_by="User"
            /label="BamHI"
     terminator      8104..8226
            /created_by="User"
            /label="T7 Tphi transcription terminator"
```

bioRxiv preprint doi: https://doi.org/10.1101/2020.03.29.013342; this version posted April 9, 2020. The copyright holder for this preprint (which was not certified by peer review) is the author/funder, who has granted bioRxiv a license to display the preprint in perpetuity. It is made available under aCC-BY-NC-ND 4.0 International license.

ORIGIN

```
   1 aactacgtca ggtggcactt ttcggggaaa tgtgcgcgga acccctattt gtttattttt
  61 ctaaatacat tcaaatatgt atccgctcat gagacaataa ccctgataaa tgcttcaata
 121 atattgaaaa aggaagagta tgagtattca acatttccgt gtcgccctta ttccctttt
 181 tgcggcattt tgccttcctg tttttgctca cccagaaacg ctggtgaaag taaaagatgc
 241 tgaagatcag ttgggtgcac gagtgggtta catcgaactg gatctcaaca gcggtaagat
 301 ccttgagagt tttcgccccg aagaacgttt cccaatgatg agcactttta aagttctgct
 361 atgtggcgcg gtattatccc gtgttgacgc cgggcaagag caactcggtc gccgcataca
 421 ctattctcag aatgacttgg ttgagtactc accagtcaca gaaaagcatc ttacggatgg
 481 catgacagta agagaattat gcagtgctgc cataaccatg agtgataaca ctgcggccaa
 541 cttacttctg acaacgatcg gaggaccgaa ggagctaacc gcttttttgc acaacatggg
 601 ggatcatgta actcgccttg atcgttggga accggagctg aatgaagcca taccaaacga
 661 cgagcgtgac accacgatgc ctgtagcaat ggcaacaacg ttgcgcaaac tattaactgg
 721 cgaactactt actctagctt cccggcaaca attaatagac tggatggagg cggataaagt
 781 tgcaggacca cttctgcgct cggcccttcc ggctggctgg tttattgctg ataaatctgg
 841 agccggtgag cgtgggtctc gcggtatcat tgcagcactg gggccagatg gtaagccctc
 901 ccgtatcgta gttatctaca cgacggggag tcaggcaact atggatgaac gaaatagaca
 961 gatcgctgag ataggtgcct cactgattaa gcattggtaa ctgtcagacc aagtttactc
1021 atatatactt tagattgatt taccccggtt gataatcaga aaagccccaa aaacaggaag
1081 attgtataag caaatattta aattgtaaac gttaatattt tgttaaaatt cgcgttaaat
1141 ttttgttaaa tcagctcatt ttttaaccaa taggccgaaa tcggcaaaat cccttataaa
1201 tcaaaagaat agcccgagat agggttgagt gttgttccag tttggaacaa gagtccacta
1261 ttaaagaacg tggactccaa cgtcaaaggg cgaaaaaccg tctatcaggg cgatggccca
1321 ctacgtgaac catcacccaa atcaagtttt ttggggtcga ggtgccgtaa agcactaaat
1381 cggaacccta aagggagccc ccgatttaga gcttgacggg gaaagccggc gaacgtggcg
1441 agaaaggaag ggaagaaagc gaaaggagcg ggcgctaggg cgctggcaag tgtagcggtc
1501 acgctgcgcg taaccaccac acccgccgcg cttaatgcgc cgctacaggg cgcgtaaaag
1561 gatctaggtg aagatccttt ttgataatct catgaccaaa atcccttaac gtgagttttc
1621 gttccactga gcgtcagacc ccgtagaaaa gatcaaagga tcttcttgag atcctttttt
1681 tctgcgcgta atctgctgct tgcaaacaaa aaaaccaccg ctaccagcgg tggtttgttt
1741 gccggatcaa gagctaccaa ctctttttcc gaaggtaact ggcttcagca gagcgcagat
1801 accaaatact gtccttctag tgtagccgta gttaggccac cacttcaaga actctgtagc
1861 accgcctaca tacctcgctc tgctaatcct gttaccagtg gctgctgcca gtggcgataa
1921 gtcgtgtctt accgggttgg actcaagacg atagttaccg gataaggcgc agcggtcggg
1981 ctgaacgggg ggttcgtgca cacagcccag cttggagcga acgacctaca ccgaactgag
2041 atacctacag cgtgagctat gagaaagcgc cacgcttccc gaagggagaa aggcggacag
2101 gtatccggta agcggcaggg tcggaacagg agagcgcacg agggagcttc caggggggaaa
2161 cgcctggtat ctttatagtc ctgttgggtt tcgccacctc tgacttgagc gtcgattttt
2221 gtgatgctcg tcaggggggc ggagcctatg gaaaaacgcc agcaacgcgg cctttttacg
2281 gttcctggcc ttttgctggc cttttgctca catgttcttt cctgcgttat cccctgattc
2341 tgtggataac cgtattaccg cctttgagtg agctgatacc gctcgccgca gccgaacgac
2401 cgagcgcagc gagtcagtga gcgaggaagc tatggtgcac tctcagtaca atctgctctg
2461 atgccgcata gttaagccag tatacactcc gctatcgcta cgtgactggg tcatggctgc
2521 gccccgacac ccgccaacac ccgctgacgc gccctgacgg gcttgtctgc tcccggcatc
```

bioRxiv preprint doi: https://doi.org/10.1101/2020.03.29.013342; this version posted April 9, 2020. The copyright holder for this preprint (which was not certified by peer review) is the author/funder, who has granted bioRxiv a license to display the preprint in perpetuity. It is made available under aCC-BY-NC-ND 4.0 International license.

2581 cgcttacaga caagctgtga ccgtctccgg gagctgcatg tgtcagaggt tttcaccgtc
2641 atcaccgaaa cgcgcgaggc agctgcggta aagctcatca gcgtggtcgt gcagcgattc
2701 acagatgtct gcctgttcat ccgcgtccag ctcgttgagt ttctccagaa gcgttaatgt
2761 ctggcttctg ataaagcggg ccatgttaag ggcggttttt tcctgtttgg tcactgatgc
2821 ctccgtgtaa gggggatttc tgttcatggg ggtaatgata ccgatgaaac gagagaggat
2881 gctcacgata cgggttactg atgatgaaca tgcccggtta ctggaacgtt gtgagggtaa
2941 acaactggcg gtatggatgc ggcgggacca gagaaaaatc actcagggtc aatgccagcc
3001 gaacgccagc aagacgtagc ccagcgcgtc ggccgccatg ccggcgataa tggcctgctt
3061 ctcgccgaaa cgtttggtgg cgggaccagt gacgaaggct tgagcgaggg cgtgcaagat
3121 tccgaatacc gcaagcgaca ggccgatcat cgtcgcgctc cagcgaaagc ggtcctcgcc
3181 gaaaatgacc cagagcgctg ccggcacctg tcctacgagt tgcatgataa agaagacagt
3241 cataagtgcg gcgacgatag tcatgccccg cgcccaccgg aaggagctga ctgggttgaa
3301 ggctctcaag ggcatcggtc gagatcccgg tgcctaatga gtgagctaac ttacattaat
3361 tgcgttgcgc tcactgcccg ctttccagtc gggaaacctg tcgtgccagc tgcattaatg
3421 aatcggccaa cgcgcgggga gaggcggttt gcgtattggg cgccagggtg gtttttcttt
3481 tcaccagtga gacgggcaac agctgattgc ccttcaccgc ctggccctga gagagttgca
3541 gcaagcggtc cacgctggtt tgccccagca ggcgaaaatc ctgtttgatg gtggttaacg
3601 gcgggatata acatgagctg tcttcggtat cgtcgtatcc cactaccgag atgtccgcac
3661 caacgcgcag cccggactcg gtaatggcgc gcattgcgcc cagcgccatc tgatcgttgg
3721 caaccagcat cgcagtggga acgatgccct cattcagcat ttgcatggtt tgttgaaaac
3781 cggacatggc actccagtcg ccttcccgtt ccgctatcgg ctgaatttga ttgcgagtga
3841 gatatttatg ccagccagcc agacgcggac gcgccgagac agaacttaat gggcccgcta
3901 acagcgcgat ttgctggtga cccaatgcga ccagatgctc cacgcccagt cgcgtaccgt
3961 cttcatggga gaaaataata ctgttgatgg gtgtctggtc agagacatca agaaataacg
4021 ccggaacatt agtgcaggca gcttccacag caatggcatc ctggtcatcc agcggatagt
4081 taatgatcag cccactgacg cgttgcgcga gaagattgtg caccgccgct ttacaggctt
4141 cgacgccgct tcgttctacc atcgacacca ccacgctggc acccagttga tcggcgcgag
4201 atttaatcgc cgcgacaatt tgcgacggcg cgtgcagggc cagactggag gtggcaacgc
4261 caatcagcaa cgactgtttg cccgccagtt gttgtgccac gcggttggga atgtaattca
4321 gctccgccat cgccgcttcc actttttccc gcgttttcgc agaaacgtgg ctggcctggt
4381 tcaccacgcg ggaaacggtc tgataagaga caccggcata ctctgcgaca tcgtataacg
4441 ttactggttt cacattcacc accctgaatt gactctcttc cgggcgctat catgccatac
4501 cgcgaaaggt tttgcgccat tcgatggtgt ccgggatctc gacgctctcc cttatgcgac
4561 tcctgcatta ggaagcagcc cagtagtagg ttgaggccgt tgagcaccgc cgccgcaagg
4621 aatggtgcat gccggcatgc cgccctttcg tcttcaagaa ttaattccca attccccagg
4681 catcaaataa aacgaaaggc tcagtcgaaa gactgggcct ttcgttttat ctgttgtttg
4741 tcggtgaacg ctctcctgag taggacaaat ccgccgggag cggatttgaa cgttgcgaag
4801 caacggcccg gagggtggcg ggcaggacgc ccgccataaa ctgccaggaa ttaattcccc
4861 aggcatcaaa taaaacgaaa ggctcagtcg aaagactggg cctttcgttt tatctgttgt
4921 ttgtcggtga acgctctcct gagtaggaca aatccgccgg gagcggattt gaacgttgcg
4981 aagcaacggc ccggagggtg gcgggcagga cgcccgccat aaactgccag gaattaattc
5041 cccaggcatc aaataaaacg aaaggctcag tcgaaagact gggcctttcg ttttatctgt
5101 tgtttgtcgg tgaacgctct cctgagtagg acaaatccgc cgggagcgga tttgaacgtt
5161 gcgaagcaac ggcccggagg gtggcgggca ggacgcccgc cataaactgc caggaattaa

bioRxiv preprint doi: https://doi.org/10.1101/2020.03.29.013342; this version posted April 9, 2020. The copyright holder for this preprint (which was not certified by peer review) is the author/funder, who has granted bioRxiv a license to display the preprint in perpetuity. It is made available under aCC-BY-NC-ND 4.0 International license.

5221 ttccccaggc atcaaataaa acgaaaggct cagtcgaaag actgggcctt tcgttttatc
5281 tgttgtttgt cggtgaacgc tctcctgagt aggacaaatc cgccgggagc ggatttgaac
5341 gttgcgaagc aacggcccgg agggtggcgg gcaggacgcc cgccataaac tgccaggaat
5401 taattcccca ggcatcaaat aaaacgaaag gctcagtcga aagactgggc ctttcgtttt
5461 atctgttgtt tgtcggtgaa cgctctcctg agtaggacaa atccgccggg agcggatttg
5521 aacgttgcga agcaacggcc cggagggtgg cgggcaggac gcccgccata aactgccagg
5581 aattggggat cggaattaat tcccggttta aaccggggat ctcgatcccg cgaaattaat
5641 acgactcact atagggggaat tgtgagcgga taacaattcc cctctagaaa taattttgtt
5701 taactttaag aaggagatat acatatgatt cttgacacgg attacatcac ggaagacggc
5761 aagccggtta tccgtatttt caagaaagaa aacggcgaat tcaagattga atacgatcgg
5821 acatttgaac cgtacctgta cgctctcctc aaggatgata gcgcaatcga agaagtgaaa
5881 aaaatcaccg cagagcggca tggcacagtg gtaacagtta agcgggtcga gaaagtgcag
5941 aagaagttct taggccggcc agtcgaagta tggaaattat acttcacaca tccacaggac
6001 gttccggcga tcatggataa gattcgggag catccggcgg taatcgatat ctatgaatac
6061 gatattccgt tcgctattcg ctaccttatt gacaaaggtt tagttccaat ggagggtgat
6121 gaggaactta aactgttagc attcgatatc gaaacacttt atcacgaagg tgaagagttt
6181 gccgaaggtc cgattttaat gatctcgtac gccgatgaag aaggcgcacg cgtaattacg
6241 tggaaaaatg tggacctccc gtacgtagac gtagtgagca ctgagcgcga gatgattaaa
6301 cgtttccttc gggtagtaaa agaaaaagac ccagacgtgc tgattacgta taacggcgac
6361 aactttgatt ttgcctatct caagaagcgt tgcgaaaagt taggcattaa tttcgccctg
6421 ggtcgggacg gttcagagcc gaaaattcag cggatgggcg accgctttgc tgtggaggta
6481 aaaggtcgca tccatttcga tttatatccg gttatccggc gcaccatcaa cttgccgact
6541 tacacacttg aagcagttta cgaagcggtg ttcggccaac caaaagaaaa ggtttatgcc
6601 gaggagatta ccaccgcatg ggaaactggc gaaaacttgg agcgggtggc tcggtattcc
6661 atggaagatg ccaaggtgac ctacgaactg ggcaaagagt ttttaccgat ggaagcacaa
6721 ttaagccgcc ttattggtca gtccctctgg gatgtgtcgc gttcttcaac gggcaattta
6781 gtcgaatggt ttcttcttcg gaaagcgtac gagcgtaacg agcttgctcc aaataagcca
6841 gacgaaaaag aattggctcg gcgccatcag tcacatgagg gcggctacat taaggagcca
6901 gaacggggct tgtgggagaa catcgtctac cttgattttc ggtctcttta tccgtctatt
6961 atcatcacac ataacgtctc gccagatacc ctgaaccgtg aaggctgtaa agaatatgat
7021 gtggcaccac aggtcggcca tcgtttttgt aaagacttcc cgggcttcat tccatctctt
7081 ctgggtgatt tgttagaaga gcgtcaaaag atcaagaaac gtatgaaagc gacaattgac
7141 ccaattgaac gcaaattact tgattaccgt cagcgtgcaa tcaagatcct cgcgaactct
7201 ctgtacggtt attacggcta cgcacgcgcc cggtggtatt gcaaagaatg tgcagaatca
7261 gtcattgctt ggggtcggga gtacctgacc atgacgatta aggaaattga ggagaaatac
7321 ggtttcaagg tcatctatag tgacacggat ggtttctttg caacgattcc aggtgcggac
7381 gcagaaactg taaagaaaaa ggcaatggag ttcttgaagt atattaatgc gaagttgcca
7441 ggcgccctgg aattagagta cgaaggtttt tataagcgtg gcctgttcgt gacaaagaag
7501 aaatacgcgg taattgacga ggaaggcaag atcacaactc gtggcttgga aattgttcgt
7561 cgcgattgga gcgagatcgc aaaggagacc caagctcgtg tgttggaggc cctcctgaag
7621 gatggtgacg tcgaaaaagc cgtacgcatc gttaaggagg ttacagagaa gcttagcaag
7681 tatgaggtcc caccagagaa acttgttatt cataaacaaa tcactcgcga ccttaaagac
7741 tataaggcca ctggtccaca cgtcgccgta gcaaagcggc ttgcggctcg gggcgtcaag
7801 attcggccag gcacggttat tagttacatc gtcctcaaag gctcaggccg gattgttgat

bioRxiv preprint doi: https://doi.org/10.1101/2020.03.29.013342; this version posted April 9, 2020. The copyright holder for this preprint (which was not certified by peer review) is the author/funder, who has granted bioRxiv a license to display the preprint in perpetuity. It is made available under aCC-BY-NC-ND 4.0 International license.

```
   7861 cgcgcgattc catttgatga atttgatccg acgaagcata aatatgatgc ggaatattac
   7921 attgaaaaac aggttctgcc ggcggtggag cgcatcttac gtgcgttcgg ctatcgcaag
   7981 gaggatttgc ggtaccagaa aactcgtcaa gtcggtttga gtgcccgtct gaagccgaaa
   8041 ggtaccctcg agggatccag ccatcaccat caccatcact gataagcggc cgcattgatc
   8101 cggctgctaa caaagcccga aaggaagctg agttggctgc tgccaccgct gagcaataac
   8161 tagcataacc ccttggggcc tctaaacggg tcttgagggg ttttttgctg aaaggaggaa
   8221 ctatatccgg at
//
```

Table S1. GenBank format of pET_RTX-6xHis

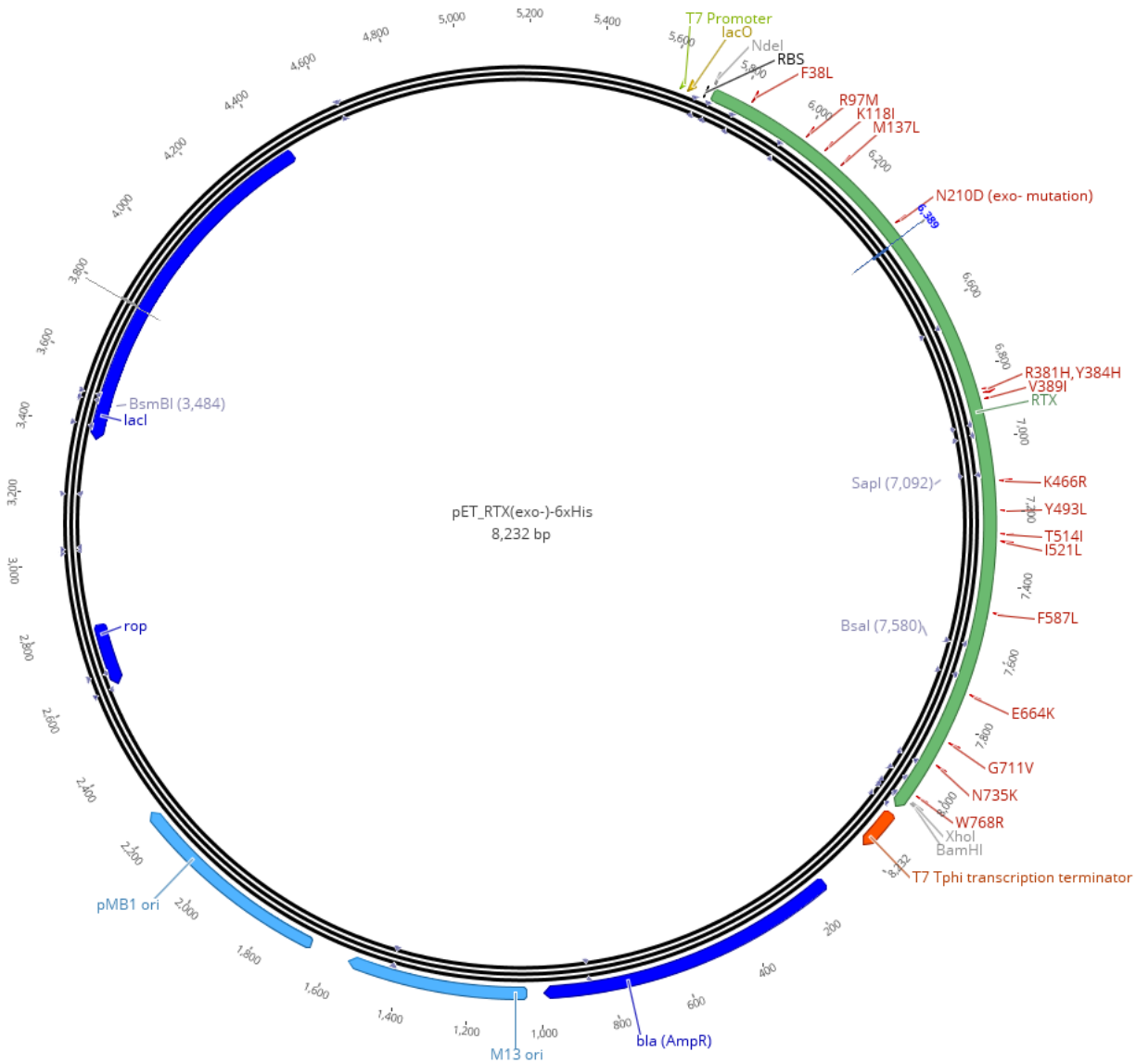

Figure S2. Plasmid map pET_RTX(exo-)-6xHis

```
LOCUS       pET_RTX(exo-)-6x       8232 bp    DNA     circular UNA 26-MAR-2020
DEFINITION  A new nucleotide sequence entered manually.
```

bioRxiv preprint doi: https://doi.org/10.1101/2020.03.29.013342; this version posted April 9, 2020. The copyright holder for this preprint (which was not certified by peer review) is the author/funder, who has granted bioRxiv a license to display the preprint in perpetuity. It is made available under aCC-BY-NC-ND 4.0 International license.

```
ACCESSION   urn.local...28-bq4yik3
VERSION     urn.local...28-bq4yik3
KEYWORDS    .
SOURCE
  ORGANISM
          .
FEATURES             Location/Qualifiers
     gene            140..1000
                     /created_by="User"
                     /label="bla (AmpR)"
     rep_origin      1042..1555
                     /created_by="User"
                     /modified_by="User"
                     /label="M13 ori"
     rep_origin      1666..2254
                     /created_by="User"
                     /modified_by="User"
                     /label="pMB1 ori"
     gene            complement(2623..2814)
                     /created_by="User"
                     /label="rop"
     gene            complement(3371..4453)
                     /created_by="User"
                     /label="lacI"
     promoter        5637..5654
                     /created_by="User"
                     /label="T7 Promoter"
     operon          5656..5680
                     /created_by="User"
                     /label="lacO"
     RBS             5708..5714
                     /created_by="User"
                     /label="RBS"
     misc_feature    5722..5727
                     /created_by="User"
                     /modified_by="User"
                     /label="NdeI"
     CDS             5725..8085
                     /created_by="User"
                     /modified_by="User"
                     /label="RTX"
     misc_difference 5836..5838
                     /created_by="User"
                     /label="F38L"
```

bioRxiv preprint doi: https://doi.org/10.1101/2020.03.29.013342; this version posted April 9, 2020. The copyright holder for this preprint (which was not certified by peer review) is the author/funder, who has granted bioRxiv a license to display the preprint in perpetuity. It is made available under aCC-BY-NC-ND 4.0 International license.

```
misc_difference 6013..6015
            /created_by="User"
            /label="R97M"
misc_difference 6076..6078
            /created_by="User"
            /modified_by="User"
            /label="K118I"
misc_difference 6133..6135
            /created_by="User"
            /label="M137L"
misc_difference 6352..6354
            /created_by="User"
            /label="N210D (exo- mutation)"
misc_difference 6865..6867
            /created_by="User"
            /label="R381H"
misc_difference 6874..6876
            /created_by="User"
            /label="Y384H"
misc_difference 6889..6891
            /created_by="User"
            /label="V389I"
misc_difference 7120..7122
            /created_by="User"
            /label="K466R"
misc_difference 7201..7203
            /created_by="User"
            /label="Y493L"
misc_difference 7264..7266
            /created_by="User"
            /label="T514I"
misc_difference 7285..7287
            /created_by="User"
            /label="I521L"
misc_difference 7483..7485
            /created_by="User"
            /label="F587L"
misc_difference 7714..7716
            /created_by="User"
            /label="E664K"
misc_difference 7855..7857
            /created_by="User"
            /label="G711V"
misc_difference 7927..7929
```

bioRxiv preprint doi: https://doi.org/10.1101/2020.03.29.013342; this version posted April 9, 2020. The copyright holder for this preprint (which was not certified by peer review) is the author/funder, who has granted bioRxiv a license to display the preprint in perpetuity. It is made available under aCC-BY-NC-ND 4.0 International license.

```
                /created_by="User"
                /label="N735K"
     misc_difference 8026..8028
                /created_by="User"
                /label="W768R"
     misc_feature    8047..8052
                /created_by="User"
                /label="XhoI"
     misc_feature    8053..8058
                /created_by="User"
                /label="BamHI"
     terminator      8104..8226
                /created_by="User"
                /label="T7 Tphi transcription terminator"
ORIGIN
        1 aactacgtca ggtggcactt ttcggggaaa tgtgcgcgga acccctattt gtttattttt
       61 ctaaatacat tcaaatatgt atccgctcat gagacaataa ccctgataaa tgcttcaata
      121 atattgaaaa aggaagagta tgagtattca acatttccgt gtcgccctta ttccctttt
      181 tgcggcattt tgccttcctg tttttgctca cccagaaacg ctggtgaaag taaaagatgc
      241 tgaagatcag ttgggtgcac gagtgggtta catcgaactg gatctcaaca gcggtaagat
      301 ccttgagagt tttcgccccg aagaacgttt cccaatgatg agcactttta aagttctgct
      361 atgtggcgcg gtattatccc gtgttgacgc cgggcaagag caactcggtc gccgcataca
      421 ctattctcag aatgacttgg ttgagtactc accagtcaca gaaaagcatc ttacggatgg
      481 catgacagta agagaattat gcagtgctgc cataaccatg agtgataaca ctgcggccaa
      541 cttacttctg acaacgatcg gaggaccgaa ggagctaacc gctttttttgc acaacatggg
      601 ggatcatgta actcgccttg atcgttggga accggagctg aatgaagcca taccaaacga
      661 cgagcgtgac accacgatgc ctgtagcaat ggcaacaacg ttgcgcaaac tattaactgg
      721 cgaactactt actctagctt cccggcaaca attaatagac tggatggagg cggataaagt
      781 tgcaggacca cttctgcgct cggcccttcc ggctggctgg tttattgctg ataaatctgg
      841 agccggtgag cgtgggtctc gcggtatcat tgcagcactg gggccagatg gtaagccctc
      901 ccgtatcgta gttatctaca cgacggggag tcaggcaact atggatgaac gaaatagaca
      961 gatcgctgag ataggtgcct cactgattaa gcattggtaa ctgtcagacc aagtttactc
     1021 atatatactt tagattgatt taccccggtt gataatcaga aaagccccaa aaacaggaag
     1081 attgtataag caaatattta aattgtaaac gttaatattt tgttaaaatt cgcgttaaat
     1141 ttttgttaaa tcagctcatt ttttaaccaa taggccgaaa tcggcaaaat cccttataaa
     1201 tcaaaagaat agcccgagat agggttgagt gttgttccag tttggaacaa gagtccacta
     1261 ttaaagaacg tggactccaa cgtcaaaggg cgaaaaaccg tctatcaggg cgatggccca
     1321 ctacgtgaac catcacccaa atcaagtttt ttggggtcga ggtgccgtaa agcactaaat
     1381 cggaacccta aagggagccc ccgatttaga gcttgacggg gaaagccggc gaacgtggcg
     1441 agaaaggaag ggaagaaagc gaaaggagcg ggcgctaggg cgctggcaag tgtagcggtc
     1501 acgctgcgcg taaccaccac acccgccgcg cttaatgcgc cgctacaggg cgcgtaaaag
     1561 gatctaggtg aagatccttt ttgataatct catgaccaaa atcccttaac gtgagttttc
     1621 gttccactga gcgtcagacc ccgtagaaaa gatcaaagga tcttcttgag atcctttttt
     1681 tctgcgcgta atctgctgct tgcaaacaaa aaaaccaccg ctaccagcgg tggtttgttt
```

bioRxiv preprint doi: https://doi.org/10.1101/2020.03.29.013342; this version posted April 9, 2020. The copyright holder for this preprint (which was not certified by peer review) is the author/funder, who has granted bioRxiv a license to display the preprint in perpetuity. It is made available under aCC-BY-NC-ND 4.0 International license.

1741 gccggatcaa gagctaccaa ctctttttcc gaaggtaact ggcttcagca gagcgcagat
1801 accaaatact gtccttctag tgtagccgta gttaggccac cacttcaaga actctgtagc
1861 accgcctaca tacctcgctc tgctaatcct gttaccagtg gctgctgcca gtggcgataa
1921 gtcgtgtctt accgggttgg actcaagacg atagttaccg gataaggcgc agcggtcggg
1981 ctgaacgggg ggttcgtgca cacagcccag cttggagcga acgacctaca ccgaactgag
2041 atacctacag cgtgagctat gagaaagcgc cacgcttccc gaagggagaa aggcggacag
2101 gtatccggta agcggcaggg tcggaacagg agagcgcacg agggagcttc caggggggaaa
2161 cgcctggtat ctttatagtc ctgttgggtt tcgccacctc tgacttgagc gtcgattttt
2221 gtgatgctcg tcaggggggc ggagcctatg gaaaaacgcc agcaacgcgg cctttttacg
2281 gttcctggcc ttttgctggc cttttgctca catgttcttt cctgcgttat cccctgattc
2341 tgtggataac cgtattaccg cctttgagtg agctgatacc gctcgccgca gccgaacgac
2401 cgagcgcagc gagtcagtga gcgaggaagc tatggtgcac tctcagtaca atctgctctg
2461 atgccgcata gttaagccag tatacactcc gctatcgcta cgtgactggg tcatggctgc
2521 gccccgacac ccgccaacac ccgctgacgc gccctgacgg gcttgtctgc tcccggcatc
2581 cgcttacaga caagctgtga ccgtctccgg gagctgcatg tgtcagaggt tttcaccgtc
2641 atcaccgaaa cgcgcgaggc agctgcggta aagctcatca gcgtggtcgt gcagcgattc
2701 acagatgtct gcctgttcat ccgcgtccag ctcgttgagt ttctccagaa gcgttaatgt
2761 ctggcttctg ataaagcggg ccatgttaag ggcggttttt tcctgtttgg tcactgatgc
2821 ctccgtgtaa gggggatttc tgttcatggg ggtaatgata ccgatgaaac gagagaggat
2881 gctcacgata cgggttactg atgatgaaca tgcccggtta ctggaacgtt gtgagggtaa
2941 acaactggcg gtatggatgc ggcgggacca gagaaaaatc actcagggtc aatgccagcc
3001 gaacgccagc aagacgtagc ccagcgcgtc ggccgccatg ccggcgataa tggcctgctt
3061 ctcgccgaaa cgtttggtgg cgggaccagt gacgaaggct tgagcgaggg cgtgcaagat
3121 tccgaatacc gcaagcgaca ggccgatcat cgtcgcgctc cagcgaaagc ggtcctcgcc
3181 gaaaatgacc cagagcgctg ccggcacctg tcctacgagt tgcatgataa agaagacagt
3241 cataagtgcg gcgacgatag tcatgccccg cgcccaccgg aaggagctga ctgggttgaa
3301 ggctctcaag ggcatcggtc gagatcccgg tgcctaatga gtgagctaac ttacattaat
3361 tgcgttgcgc tcactgcccg ctttccagtc gggaaacctg tcgtgccagc tgcattaatg
3421 aatcggccaa cgcgcgggga gaggcggttt gcgtattggg cgccagggtg gtttttcttt
3481 tcaccagtga gacgggcaac agctgattgc ccttcaccgc ctggccctga gagagttgca
3541 gcaagcggtc cacgctggtt tgccccagca ggcgaaaatc ctgtttgatg gtggttaacg
3601 gcgggatata acatgagctg tcttcggtat cgtcgtatcc cactaccgag atgtccgcac
3661 caacgcgcag cccggactcg gtaatggcgc gcattgcgcc cagcgccatc tgatcgttgg
3721 caaccagcat cgcagtggga acgatgccct cattcagcat ttgcatggtt tgttgaaaac
3781 cggacatggc actccagtcg ccttcccgtt ccgctatcgg ctgaatttga ttgcgagtga
3841 gatatttatg ccagccagcc agacgcggac gcgccgagac agaacttaat gggcccgcta
3901 acagcgcgat ttgctggtga cccaatgcga ccagatgctc cacgcccagt cgcgtaccgt
3961 cttcatggga gaaaataata ctgttgatgg gtgtctggtc agagacatca agaaataacg
4021 ccggaacatt agtgcaggca gcttccacag caatggcatc ctggtcatcc agcggatagt
4081 taatgatcag cccactgacg cgttgcgcga gaagattgtg caccgccgct ttacaggctt
4141 cgacgccgct tcgttctacc atcgacacca ccacgctggc acccagttga tcggcgcgag
4201 atttaatcgc cgcgacaatt tgcgacggcg cgtgcagggc cagactggag gtggcaacgc
4261 caatcagcaa cgactgtttg cccgccagtt gttgtgccac gcggttggga atgtaattca
4321 gctccgccat cgccgcttcc actttttccc gcgttttcgc agaaacgtgg ctggcctggt

bioRxiv preprint doi: https://doi.org/10.1101/2020.03.29.013342; this version posted April 9, 2020. The copyright holder for this preprint (which was not certified by peer review) is the author/funder, who has granted bioRxiv a license to display the preprint in perpetuity. It is made available under aCC-BY-NC-ND 4.0 International license.

4381 tcaccacgcg ggaaacggtc tgataagaga caccggcata ctctgcgaca tcgtataacg
4441 ttactggttt cacattcacc accctgaatt gactctcttc cgggcgctat catgccatac
4501 cgcgaaaggt tttgcgccat tcgatggtgt ccgggatctc gacgctctcc cttatgcgac
4561 tcctgcatta ggaagcagcc cagtagtagg ttgaggccgt tgagcaccgc cgccgcaagg
4621 aatggtgcat gccggcatgc cgccctttcg tcttcaagaa ttaattccca attccccagg
4681 catcaaataa aacgaaaggc tcagtcgaaa gactgggcct ttcgttttat ctgttgtttg
4741 tcggtgaacg ctctcctgag taggacaaat ccgccgggag cggatttgaa cgttgcgaag
4801 caacggcccg gagggtggcg ggcaggacgc ccgccataaa ctgccaggaa ttaattcccc
4861 aggcatcaaa taaaacgaaa ggctcagtcg aaagactggg cctttcgttt tatctgttgt
4921 ttgtcggtga acgctctcct gagtaggaca aatccgccgg gagcggattt gaacgttgcg
4981 aagcaacggc ccggagggtg gcgggcagga cgcccgccat aaactgccag gaattaattc
5041 cccaggcatc aaataaaacg aaaggctcag tcgaaagact gggcctttcg ttttatctgt
5101 tgtttgtcgg tgaacgctct cctgagtagg acaaatccgc cgggagcgga tttgaacgtt
5161 gcgaagcaac ggcccggagg gtggcgggca ggacgcccgc cataaactgc caggaattaa
5221 ttccccaggc atcaaataaa acgaaaggct cagtcgaaag actgggcctt tcgttttatc
5281 tgttgtttgt cggtgaacgc tctcctgagt aggacaaatc cgccgggagc ggatttgaac
5341 gttgcgaagc aacggcccgg agggtggcgg gcaggacgcc cgccataaac tgccaggaat
5401 taattcccca ggcatcaaat aaaacgaaag gctcagtcga aagactgggc ctttcgtttt
5461 atctgttgtt tgtcggtgaa cgctctcctg agtaggacaa atccgccggg agcggatttg
5521 aacgttgcga agcaacggcc cggagggtgg cgggcaggac gcccgccata aactgccagg
5581 aattggggat cggaattaat tcccggttta aaccggggat ctcgatcccg cgaaattaat
5641 acgactcact atagggggaat tgtgagcgga taacaattcc cctctagaaa taattttgtt
5701 taactttaag aaggagatat acatatgatt cttgacacgg attacatcac ggaagacggc
5761 aagccggtta tccgtatttt caagaaagaa aacggcgaat tcaagattga atacgatcgg
5821 acatttgaac cgtacctgta cgctctcctc aaggatgata gcgcaatcga agaagtgaaa
5881 aaaatcaccg cagagcggca tggcacagtg gtaacagtta agcgggtcga gaaagtgcag
5941 aagaagttct taggccggcc agtcgaagta tggaaattat acttcacaca tccacaggac
6001 gttccggcga tcatggataa gattcgggag catccggcgg taatcgatat ctatgaatac
6061 gatattccgt tcgctattcg ctaccttatt gacaaaggtt tagttccaat ggagggtgat
6121 gaggaactta aactgttagc attcgatatc gaaacacttt atcacgaagg tgaagagttt
6181 gccgaaggtc cgattttaat gatctcgtac gccgatgaag aaggcgcacg cgtaattacg
6241 tggaaaaatg tggacctccc gtacgtagac gtagtgagca ctgagcgcga gatgattaaa
6301 cgtttccttc gggtagtaaa agaaaaagac ccagacgtgc tgattacgta tgacggcgac
6361 aactttgatt ttgcctatct caagaagcgt tgcgaaaagt taggcattaa tttcgccctg
6421 ggtcgggacg gttcagagcc gaaaattcag cggatgggcg accgctttgc tgtggaggta
6481 aaaggtcgca tccatttcga tttatatccg gttatccggc gcaccatcaa cttgccgact
6541 tacacacttg aagcagttta cgaagcggtg ttcggccaac caaaagaaaa ggtttatgcc
6601 gaggagatta ccaccgcatg ggaaactggc gaaaacttgg agcgggtggc tcggtattcc
6661 atggaagatg ccaaggtgac ctacgaactg ggcaaagagt ttttaccgat ggaagcacaa
6721 ttaagccgcc ttattggtca gtccctctgg gatgtgtcgc gttcttcaac gggcaattta
6781 gtcgaatggt ttcttcttcg gaaagcgtac gagcgtaacg agcttgctcc aaataagcca
6841 gacgaaaaag aattggctcg gcgccatcag tcacatgagg gcggctacat taaggagcca
6901 gaacggggct tgtgggagaa catcgtctac cttgattttc ggtctcttta tccgtctatt
6961 atcatcacac ataacgtctc gccagatacc ctgaaccgtg aaggctgtaa agaatatgat

bioRxiv preprint doi: https://doi.org/10.1101/2020.03.29.013342; this version posted April 9, 2020. The copyright holder for this preprint (which was not certified by peer review) is the author/funder, who has granted bioRxiv a license to display the preprint in perpetuity. It is made available under aCC-BY-NC-ND 4.0 International license.

```
    7021 gtggcaccac aggtcggcca tcgtttttgt aaagacttcc cgggcttcat tccatctctt
    7081 ctgggtgatt tgttagaaga gcgtcaaaag atcaagaaac gtatgaaagc gacaattgac
    7141 ccaattgaac gcaaattact tgattaccgt cagcgtgcaa tcaagatcct cgcgaactct
    7201 ctgtacggtt attacggcta cgcacgcgcc cggtggtatt gcaaagaatg tgcagaatca
    7261 gtcattgctt ggggtcggga gtacctgacc atgacgatta aggaaattga ggagaaatac
    7321 ggtttcaagg tcatctatag tgacacggat ggtttctttg caacgattcc aggtgcggac
    7381 gcagaaactg taaagaaaaa ggcaatggag ttcttgaagt atattaatgc gaagttgcca
    7441 ggcgccctgg aattagagta cgaaggtttt tataagcgtg gcctgttcgt gacaaagaag
    7501 aaatacgcgg taattgacga ggaaggcaag atcacaactc gtggcttgga aattgttcgt
    7561 cgcgattgga gcgagatcgc aaaggagacc caagctcgtg tgttggaggc cctcctgaag
    7621 gatggtgacg tcgaaaaagc cgtacgcatc gttaaggagg ttacagagaa gcttagcaag
    7681 tatgaggtcc caccagagaa acttgttatt cataaacaaa tcactcgcga ccttaaagac
    7741 tataaggcca ctggtccaca cgtcgccgta gcaaagcggc ttgcggctcg gggcgtcaag
    7801 attcggccag gcacggttat tagttacatc gtcctcaaag gctcaggccg gattgttgat
    7861 cgcgcgattc catttgatga atttgatccg acgaagcata aatatgatgc ggaatattac
    7921 attgaaaaac aggttctgcc ggcggtggag cgcatcttac gtgcgttcgg ctatcgcaag
    7981 gaggatttgc ggtaccagaa aactcgtcaa gtcggtttga gtgcccgtct gaagccgaaa
    8041 ggtaccctcg agggatccag ccatcaccat caccatcact gataagcggc cgcattgatc
    8101 cggctgctaa caaagcccga aaggaagctg agttggctgc tgccaccgct gagcaataac
    8161 tagcataacc ccttggggcc tctaaacggg tcttgagggg ttttttgctg aaaggaggaa
    8221 ctatatccgg at
//
```

Table S2. GenBank format of pET_RTX(exo-)-6xHis

REFERENCES

1 Ellefson, J. W. *et al.* Synthetic evolutionary origin of a proofreading reverse transcriptase. *Science* **352**, 1590-1593, doi:10.1126/science.aaf5409 (2016).